We are IntechOpen,
the world's leading publisher of
Open Access books
Built by scientists, for scientists

4,800
Open access books available

122,000
International authors and editors

135M
Downloads

Our authors are among the

154
Countries delivered to

TOP 1%
most cited scientists

12.2%
Contributors from top 500 universities

CLARIVATE ANALYTICS
BOOK CITATION INDEX
INDEXED

WEB OF SCIENCE™

Selection of our books indexed in the Book Citation Index
in Web of Science™ Core Collection (BKCI)

Interested in publishing with us?
Contact book.department@intechopen.com

Numbers displayed above are based on latest data collected.
For more information visit www.intechopen.com

Chapter

Informational Time Causal Planes: A Tool for Chaotic Map Dynamic Visualization

Felipe Olivares, Lindiane Souza, Walter Legnani and Osvaldo A. Rosso

Abstract

In the present chapter, we made a detailed analysis of the different regimes of certain chaotic systems and their correspondence with the change in the normalized Shannon entropy, Statistical Complexity, and Fisher information measure. We construct a bidimensional plane composed of the selection of a pair of the informational tools mentioned above (a casual plane is defined), in which the different dynamical regimes appeared very clear and give more information of the underlying process. In such a way, a plane composed of the normalized Shannon entropy, statistical complexity, normalized Shannon entropy, and Fisher information measure can be applied to follow the changes in the behavior variations of the nonlinear systems.

Keywords: chaotic dynamics, statistical complexity, information theory quantifiers, Shannon entropy, Fisher information measure, Bandt-Pompe probability distribution function

1. Introduction

In the space of few decades, chaos theory has jumped from the scientific literature into the popular realm, being regarded as a new way of looking at complex systems like brains or ecosystems. It is believed that the theory manages to capture the disorganized order that pervades our world. Chaos theory is a facet of the complex system paradigm having to do with determinism randomness. As many other people before, we wish to approach it from the information theory viewpoint.

In 1959 Kolmogorov had pointed out that the probabilistic theory of information developed by Shannon could be applied to symbolic encodings of the phase space descriptions of physical non-linear dynamical systems and with line of rezoning it more or less direct characterize a process in terms of *its Kolmogorov-Sinai entropy* [1, 2]. It has been a cornerstone in the updated theory of dynamical systems that could be complimented with Pesin's theorem in 1977 [3]. With this theorem, Pesin has proven that for certain deterministic nonlinear dynamical systems exhibiting chaotic behavior, an estimation of the *Kolmogorov-Sinai entropy* can be computed as the sum of the positive Lyapunov exponents for the process.

As is well known, chaotic systems have sensitivity to initial conditions which means instability everywhere in the phase space and lead to nonperiodic motion

(chaotic time series) [4]. One of the main characteristics of this kind of systems is its capability of long-term unpredictability despite the deterministic character of the temporal trajectory. In a system undergoing chaotic motion, two closeup neighboring points in the phase space after a short time elapsed show an exponential divergence of their respective trajectories. For example, let $X_1(t)$ and $X_2(t)$ be such two points, located within a ball of radius R at time t. Further, assume that these two points cannot be resolved within the ball due to poor instrumental resolution. At some later time t', the distance between the points will typically grow to $|X_1(t') - X_2(t')| \approx |X_1(t) - X_2(t)| \exp(\Lambda |t' - t|)$, in the case of chaotic dynamics, with $\Lambda > 0$, the average of Lyapunov exponents of the system. Clearly, if $|X_1(t') - X_2(t')| > R$, the points will be apart from each other, determining a non-zero distance between them. This fact could be interpreted by a certain kind of instability which reveals some information about the phase space population that was not available at earlier times [4]. This fact contributes to think that the chaotic behavior plays a role of *information source*.

As has been shown in the literature for a many of simple nonlinear processes, the Lyapunov exponents may be computed very precisely with different algorithms. In such a way, a nonlinear dynamical system may be considered as an information source from which information-related quantifiers may help visualize relevant details of the chaotic process. The existence of simple "calibrated" sources such as the logistic map provides a means for a precise evaluation of the performance of these information quantifiers. In this communication we take advantage such fact in order to show that planar representations constructed with two information theory-based quantifiers offer one possibility of easily visualizing many interesting details of chaos characteristics, including the fine structure of chaotic attractors. We exemplified their use showing the result on two chaotic maps: the logistic map and the delayed logistic map.

2. Information theory quantifier prescription

Many systems during its functioning generate a sequence of values that can be measured constituting what is called in science as time series (TS). The analysis concerns to extract the major quantity of information of them to accomplish the understanding of the meaning of the changes characterizing different dynamical regimes. It usually computes the experimental, or when the case permits the theoretical, probability distribution function (PDF) of the regimes exhibited by the TS, from here noted as $\mathcal{X}(t)$.

The mathematical tools applied once the PDF is available receive the name of informational tools; more precisely information theory quantifiers [5], the main feature of the quantifiers is exactly quantifying the amount of information coming from the TS, originating in the dynamical system.

2.1 Shannon entropy, Fisher information measure, and statistical complexity

The concept of entropy has many interpretations arising from a wide diversity of scientific and technological fields. Among them is associated with disorder, with the volume of state space, and with a lack of information too. There are various definitions according to ways of computing this important magnitude to study the dynamics of the systems, and one of the most frequent that could be considered of foundational definition is the denominated *Shannon entropy* [6], which can be

interpreted as a measure of uncertainty. The *Shannon entropy* can be considered as one of the most representative examples of information quantifiers.

Let a continuous PDF be noted by $\rho(x)$ with $x \in \Omega \subset \mathbb{R}$ and $\int_{\Omega} \rho(x)dx = 1$; its associated *Shannon Entropy* $S[\rho]$ is defined by [7]:

$$S[\rho] = -\int_{\Omega} \rho(x)\ln(\rho(x))dx. \qquad (1)$$

This concept means a global measure of the information contained in the TS; it has a low degree of sensitivity to strong changes in the distribution originating from a small-sized region of the set Ω.

For a time series $\mathcal{X}(t) \equiv \{x_t; t = 1, ..., M\}$, a set of M measures of the observable $\mathcal{X}$ and the associated PDF, given by $P = \{p_i; i = 1, ..., N\}$, with $\sum_{i=1}^{N} p_i = 1$ and N as the number of possible states of the system under study, the *Shannon entropy* (formally *Shannon's logarithmic information*) [7] is defined by

$$S[P] = -\sum_{i=1}^{N} p_i \ln(p_i). \qquad (2)$$

Eq. (2) constitutes a function of the probability $P = \{p_i; i = 1, ..., N\}$, which is equal to zero when the outcomes of a certain experiment denoted by the index k associated with probabilities $p_k \approx 1$ will occur. Therefore, the known dynamics developed by the dynamical system under study is complete. If the knowledge of the system dynamics is minimal, all the states of the system can occur with equal probability; thus, this probability can be modeled by a uniform distribution $P_e = \{p_i = 1/N; \forall i = 1, ..., N\}$.

It is useful to define the so-called normalized Shannon entropy, denoted as $H[P]$ in which its expression is

$$H[P] = S[P]/S_{max}, \qquad (3)$$

$(0 \leq H[P] \leq 1)$ with $S_{max} = S[P_e] = \ln N$.

In order to analyze the local aspects of variations in the content of information given by a TS is extended the use of the Fisher's Information Measure, which uses the gradient content of the PDF, and a difference that means the Shannon Entropy, the FIM as can be seen from its definition given in the expression (4) reflect tiny localized perturbations. It reads [8, 9]

$$F[\rho] = \int_{\Omega} \left|\frac{\partial}{\partial x}[\rho(x)]\right|^2 / \rho(x)dx = 4\int_{\Omega} \left|\frac{\partial}{\partial x}[\psi(x)]\right|^2 dx, \qquad (4)$$

where $\psi(x) = \sqrt{\rho(x)}$.

In this sense, the Fisher information is a local information quantifier. It has various interpretations, and, among others, it can be thought of as a measure of the ability to estimate a parameter. In other cases, it is applied to calculate the amount of information that can be extracted from a TS and also as a measure of the state of disorder of a system or phenomenon [8]. The so-called Cramer-Rao bound can be considered as the most important property in which the FIM participates [9]. The local sensitivity of FIM can contribute in such cases in which the analysis necessitates an appeal to a notion of *order*. When there are certain points in the set Ω at which the PDF $\rho(x) \to 0$ is convenient to redefine the FIM

avoiding the division by $\rho(x)$, in such cases an alternative expression of can be found in [9].

The signal discretization carries a problem of loss of information. It was extended studies by several authors, for example, see [10, 11] and references therein. In particular, it entails the loss of Fisher's shift invariance, which has not been relevant in the present chapter. Taking in mind the considerations made above, the discrete normalized FIM runs over the interval [0,1] and [12] is given by

$$F[P] = F_0 \sum_{i=1}^{N-1} \left[(p_{i+1})^{1/2} - (p_i)^{1/2} \right]^2, \tag{5}$$

where the normalization constant F_0 is given by

$$F_0 = \begin{cases} 1 & \text{if } p_{i^*} = 1 \text{ for } i^* = 1 \text{ or } i^* = N \text{ and } p_i = 0 \forall i \neq i^* \\ 1/2 & \text{otherwise} \end{cases}. \tag{6}$$

The local sensitivity of FIM for discrete PDFs is reflected by the fact that the specific i-ordering of the discrete values in $P = \{p_i; i = 1, ..., N\}$ must be seriously taken into account in evaluating the sum in Eq. (5) [13]. Each term in Eq. (5) can be regarded as a kind of "distance" between two contiguous probabilities. Thus, a different ordering of the pertinent summands would lead to a different FIM value, thereby its local nature.

In a system with N different states which reach a very ordered state, we can think it generates a signal with a PDF given by $P_0 = \{p_k \cong 1, \text{ and } p_i \cong 0; \forall k \neq i = 1, ..., N\}$, as it has a Shannon entropy $S[P_0] \cong 0$ and a normalized FIM $F[P_0] \cong F_0 = 1$. In the other extreme, if the system under analysis develops a very disordered state, it is natural to assume that this particular state is described by a PDF approximated by a uniform distribution $P_e = \{p_i = 1/N; \forall i = 1, ..., N\}$, and the corresponding Shannon entropy $S[P_e] \cong S_{max} = \ln N$ while $F[P_0] \cong 0$. In certain way it is easy to understand that the general behavior of the FIM is opposite to that of the Shannon entropy.

The third information quantifier applied in this chapter is the *statistical complexity measure* (SCM) which is a global informational quantifier. All the computations made in the present work were done with the definitions introduced by López-Ruiz et al., in their seminal paper [14] with improvements advanced by Lamberti et al. [15]. For a discrete probability distribution function (PDF), $P = \{p_i; i = 1, ..., N\}$, associated with a time series (TS), this functional $C[P]$ is given by

$$C[P] = Q_J[P, P_e].H[P], \tag{7}$$

where H denotes the amount of "disorder" given by the normalized Shannon entropy (Eq. (3)) and Q_J is called "disequilibrium," defined in terms of the Jensen-Shannon divergence, given by

$$Q_J[P, P_e] = Q_0 J[P, P_e] = Q_0 \{ S[(P + P_e)/2] - S[P]/2 - S[P_e]/2 \}. \tag{8}$$

The normalization condition Q_0 for the disequilibrium corresponds to the inverse of the maximum possible value of Jensen-Shannon divergence, that is, $Q_0 = J[P_0, P_e]$:

$$Q_0 = -2 \left\{ \left(\frac{N+1}{N} \right) \ln (N+1) - \ln (2N) + \ln N \right\}^{-1}. \tag{9}$$

In this way, we have $0 \leq H[P] \leq 1$ and $0 \leq Q_J[P, P_e] \leq 1$.

The $C[P]$ quantifies the existence of correlational structures giving a measure of the complexity of a TS. In the case of perfect order or total randomness of a signal coming of a dynamical system, the value of the $C[P]$ is identically null that means the signal possesses no structure. In between these two extreme instances, a large range of possible stages of physical structure may be realized by a dynamical system. These stages should be reflected in the features of the obtained PDF and quantified by a no-null $C[P]$.

The global character of the SCM arising in that its value does not change with different orderings of the PDF. So the $C[P]$ quantifies the disorder but also the degree of correlational structures. It is evident that the SCM adopted in this work is a not a trivial function of the entropy. It has consequences in the ranges that this information quantifier can take. For a given H value, the complexity C runs on a precise range limited by a minimum C_{min} and a maximum C_{max} [16]. These extreme values depend only on the probability space dimension and, of course, on the functional form adopted by H and Q_J.

2.2 The Bandt and Pompe approach to building up a PDF

In the beginning of this section, it was mentioned that during the analysis of a TS, one of the first steps is the computation of the PDF associated. Immediately a question emerges: What is the appropriate PDF that can be computed from the TS? The regrettable answer is not unique. There is no universal nonparametric algorithm given by the statistics in the literature to do with this task.

To give light in this subject, Bandt and Pompe (BP) [17] introduce a simple and robust symbolic method that takes into account the time causality connected with dynamics of the system. They proposed to use a symbol sequence from the TS that can be constructed in a natural way. So the PDF introduced by Bandt and Pompe (BP-PDF) did not use any kind of assumption about the model, in general unknown, in which of the underlying dynamics exists. To compute the BP-PDF, the "partitions" are constructed by comparing the order of neighboring relative values in the TS rather than by apportioning amplitudes according to different levels like in the usual amplitude statistic methodology.

One problem remains linked with the lack of information associated with the temporal causality in which origins are in the computed methodologies to calculate the amplitude of the histograms. To give an answer to this problem, Kowalski and co-workers [18] using the Cressie-Read family of divergence measure showed in quantitative assessment the advantages of the BP-PDF in relation to any scheme based upon the construction of the corresponding amplitude histogram of the PDF, and also the BP-PDF brought some insight information about the dynamics of the physical problem.

Two parameters are necessary to define at the time of computing the BP-PDF, namely, the embedding dimension and the embedding delay. To clarify these crucial concepts, we will give the following details. Let TS $\mathcal{X}(t) = \{x_t; t = 1, ..., M\}$, with an embedding dimension $D > 1$ ($D \in \mathbb{N}$) and an embedding delay $\tau > 1$ ($\tau \in \mathbb{N}$); the BP pattern of order D generated by this selection of parameters shall be considered of the form

$$s \mapsto \left(x_{s-(D-1)\tau}, x_{s-(D-2)\tau}, x_{s-(D-3)\tau}, ..., x_{s-\tau}, x_s\right). \tag{10}$$

So the methodology proposed by Bandt and Pompe has as a starting point for every time s, assigned with a D-dimensional vector that results from the evaluation

of $\mathcal{X}(t)$ at times $s - (D-1)\tau, s - (D-2)\tau, ..., s - \tau, s$. It is easy to note that higher values of D imply more information about "the past" to contribute in the PDF.

Once time settled the ordinal pattern of order D related to the time sequence s, the next step is to compute the permutation pattern denoted by $\pi = (r_0, r_1, ..., r_{D-1})$ of $(0, 1, ..., D-1)$ that could be formalized by

$$x_{s-r_{(D-1)}\tau} \leq x_{s-r_{(D-2)}\tau} \leq ... \leq x_{s-r_1\tau} \leq x_{s-r_0\tau}. \tag{11}$$

At this stage of the BP-PDF procedure, the vector defined by Eq. (10) is converted into a definite symbol π. Then to get a unique result, BP considers that $r_k < r_{k-1}$ if $x_{s-r_k\tau} = x_{s-r_{k-1}\tau}$. This is justified if the values of $\{x_t\}$ have a continuous distribution so that equal values are very unusual.

Considering all the $D!$ possible orderings (permutations) π_i when embedding dimension D, their associated relative frequencies can be naturally computed according to the number of times; this sequence order is found in the TS, divided by the total number of sequences

$$p(\pi_i) = \frac{\#\{s | s \leq M - (D-1)\tau; (s) \ has \ type \ \pi_i\}}{M - (D-1)\tau}. \tag{12}$$

In Eq. (12) the symbol # (usually applied to designate the set cardinality) means "number." In such a way, an ordinal pattern probability distribution $\Pi = \{p(\pi_i); i = 1, ..., D!\}$ is constructed from the TS.

Time series amplitude information is not considered, and it is a clear disadvantage of the methodology proposed by BP, but it is compensated by the valuable information given by the intrinsic structure of the process under analysis. The scheme proposed by BP can be understood as a symbolic representation of time series by recourse to a comparison of consecutive points ($\tau = 1$) or nonconsecutive ($\tau > 1$) points allowing for an accurate empirical reconstruction of the underlying phase space, even in the presence of weak (observational and dynamical) noise [17]. It is noticeable that the ordinal-pattern's associated PDF results invariant with respect to nonlinear monotonous transformations. Accordingly, nonlinear drifts or scaling artificially introduced by a measurement device will not modify the quantifier estimation, a nice property if one deals with experimental data (see [19]). Summing up all these advantages makes the BP methodology a better choice than conventional methods based on range partitioning.

Among other properties, we can mention the following characteristics to give reasons in the selection of the BP-PDF: (i) the reduced number of parameters needed contributes to its simplicity of implementation (D and τ the embedding length and delay, respectively), and (ii) the time required in the calculation process is in fact very short. The BP methodology has an extra advantage; it can be used to compute the PDF in TS arising in low-dimensional dynamical systems, and signals originated in a wide diversity of systems as well as chaotic, noisy, and regular reality-based ones, with a light analysis in the stationarity because there no mandatory condition to accomplish with a strong stationary assumption (for details see [17]).

Parameter D, required by the BP-PDF methodology, determines the number of accessible states which is given by $D!$. Moreover, the minimum length of the TS must satisfy the condition $M >> D!$ in order to achieve a reliable statistic and proper distinction between stochastic and deterministic dynamics [20]. The seminal work of BP [17] includes an advice on the choice of range of the parameters to compute the BP-PDF, when the selection of time lag is $\tau = 1$, and recommends the other parameter (D) to pick up on the interval $3 \leq D \leq 6$.

2.3 Ordinal patterns for deterministic processes

There is a demonstrated fact, done by Amigó et al. [21, 22], that in the case of deterministic one-dimensional maps, independently of the TS length M, *not all possible ordinal patterns*, applying BP methodology [17], can effectively give orbits in the phase space. This is a kind of a new dynamical property that means the existence of *forbidden ordinal patterns*. The proximity of patterns as well as correlation is not linked with the abovementioned property [21, 22]. So the informational quantifiers give a new characteristic in the analysis of chaotic or deterministic TS.

2.4 Causal informational planes

To characterize a given dynamical system described by a TS, we are able to use two representation spaces: (a) one with global-global characteristics called causal entropy-complexity plane ($H \times C$) and (b) one with global-local characteristics called causality Shannon-Fisher plane ($H \times F$), respectively.

The time causal nature of the Bandt and Pompe PDF gives a criterion to separate and differentiate chaotic and stochastic systems in different regions in both informational planes ($H[\Pi] \times C[\Pi]$) [23] and ($H[\Pi] \times F[\Pi]$) [24, 25]. While the global plane gives information of the complexity of a system, the local one becomes able to separate different dynamical behaviors in function of a control parameter.

3. Description of the chaotic maps

We focus our attention on two chaotic maps, namely, the logistic map and logistic map with delay.

3.1 The logistic map

One of the most used examples of deterministic chaotic systems is the logistic map. Its simplicity and easy computational implementation had been one of the most useful tools to explain chaotic behavior. It is a quadratic map $\mathcal{F} : x_n \to x_{n+1}$ [26], described by the ecologically motivated, dissipative system given by the first-order difference equation:

$$x_{n+1} = r\, x_n(1 - x_n), \qquad (13)$$

where $0 \leq x_n \leq 1$ and $0 \leq r \leq 4$ can be associated with a kind of growth rate in the population dynamics. The corresponding Lyapunov exponent can be evaluated numerically [26] via

$$\Lambda(r) = \lim_{N \to \infty} \frac{1}{N} \sum_{n=0}^{N-1} \ln |r(1 - 2x_n)|, \qquad (14)$$

where N is the number of iterations. **Figure 1a** and **1b** displays the well-known bifurcation diagram and the corresponding Lyapunov exponent $\Lambda(r)$, respectively, as a function of the parameter $3.4 \leq r \leq 4.0$ with $\Delta r = 0.0005$. We evaluated numerically the logistic map starting from a random initial condition in the interval $0 < x_0 < 0.5$. The first $N_0 = 10^5$ iterations are disregarded (transitory states), and the next $N = 10^6$ ones are used for Lyapunov evaluation (Eq. (14)) and information theory quantifiers (Eqs. (3), (5), and (7)).
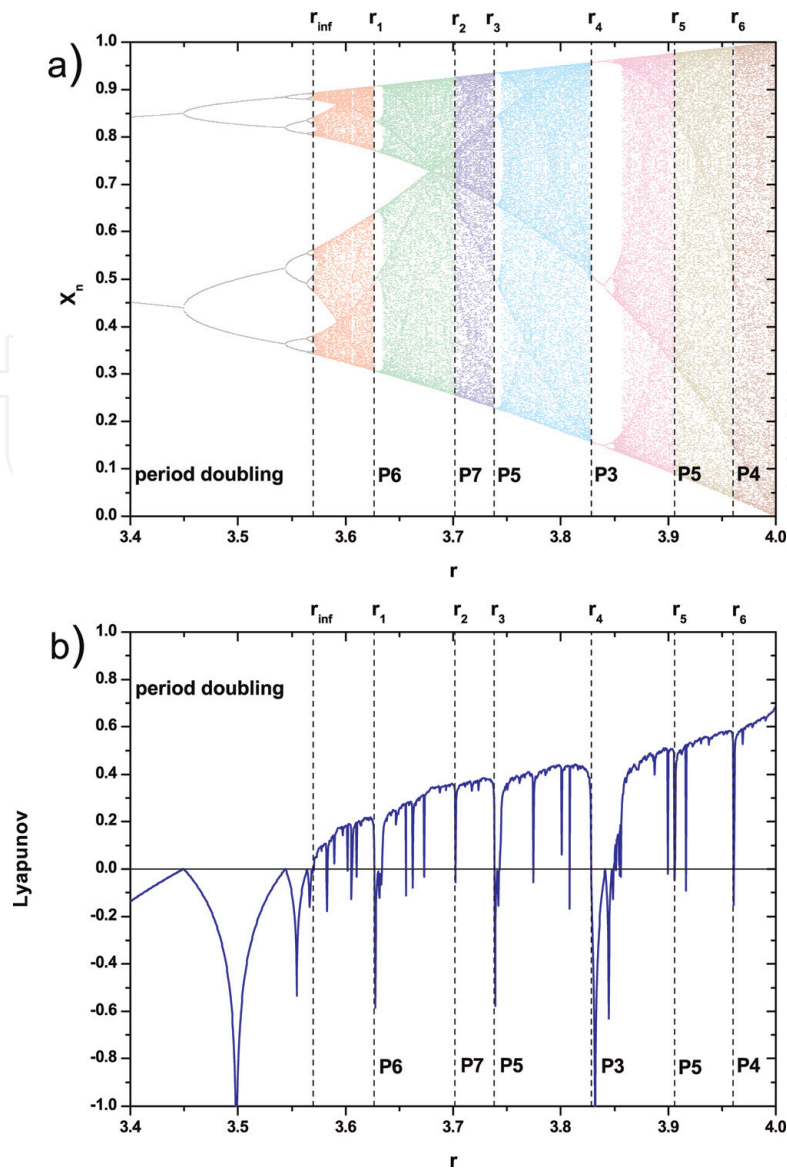
Figure 1.
(a) Bifurcation diagram and (b) Lyapunov exponent Λ for the logistic map as function of parameter r
($\Delta r = 0.0005$). The vertical segment lines delimited the different dynamical windows described in the text.

In the bifurcation diagram (**Figure 1a**), for fixed r, one appreciates that a periodic orbit consists of a countable set of points, while a chaotic attractor fills out dense bands within the unit interval. For $r \in [0, 1)$, one detects stable behavior $x_n = 0$. For $r \in [1, 3)$, there exist only a single steady-state solution given by $x_n = 1 - 1/r$. Increasing the control parameter, for $r \in [3, r_\infty)$, forces the system to undergo period-doubling bifurcations. Cycles of periods 2, 4, 8, 16, 32, etc. occur, and, if r_n denotes the values of r for which a 2^n cycle first appears, succesive r_ns converge to the limiting value $r_\infty \approx 3.5699456$ [26]. The value r_∞ splits the final-state diagram into two distinct parts: (a) the period-doubling zone on the left and (b) an area governed mainly by increasing chaotic behavior on the right. From **Figure 1b**, we see that period-doubling zone $r \in [3, r_\infty)$ Lyapunov are $\Lambda(r) \leq 0$, approximating to zero at each period-doubling bifurcation. The onset of chaos is apparent at r_∞ where Λ becomes positive for the first time. For $r = 4$ the iterates of the logistic map are represented by a random-looking distribution of dots which vertically span the range $x_n \in [0, 1]$, that is, complete developed chaos. For $r > r_\infty$ the Lyapunov exponent increases globally (see **Figure 1b**), except for dips one sees in the windows of periodic behavior. In the chaotic regime $r \in [r_\infty, 4]$, the period is

infinitely long, and finite regions of the interval are visited by the orbits. Many periodic windows are observed, and all possible periods are represented, but the width of the window decreases as the period increases. Periodic windows suddenly appear as r increases, and they contain their own periodic-doubling route toward chaos. These facts exhibit the self-similar nature of the logistic map.

In **Figure 1a** and **1b**, we marked eight zones in order to analyze the logistic map behavior. They are *Zone 1*, $r \in [3.4, r_\infty)$ which corresponds to the period-doubling zone; *Zone 2*, $r \in [r_\infty, r_1)$, with $r_1 = 3.626557$, which corresponds to the start of periodic window of period 6; *Zone 3*, $r \in [r_1, r_2)$, with $r_2 = 3.701645$, which corresponds to the start of periodic window of period 7; *Zone 4*, $r \in [r_2, r_3)$, with $r_3 = 3.738177$, which corresponds to the start of periodic window of period 5; *Zone 5*, $r \in [r_3, r_4)$, with $r_4 = 3.828427$, which corresponds to the start of periodic window of period 3; *Zone 6*, $r \in [r_4, r_5)$, the largest periodic window, with $r_5 = 3.905573$, which corresponds to the start of periodic window of period 5; *Zone 7*, $r \in [r_5, r_6)$, with $r_6 = 3.960108$, which corresponds to the start of periodic window of period 4; and *Zone 8*, $r \in [r_6, 4]$, with $r = 4$ for fully developed chaos.

Periodic windows "interrupt" chaotic behavior in noticeable fashion. At the beginning of a window, there is a sudden and dramatic change in the long-term behavior of the logistic map. Consider, for example, the behavior for $r \geq r_4$ corresponding to the beginning of a period 3 window. We see three miniature copies of the whole final-state diagram (**Figure 1a**), and, indeed, we can reproduce the entire scenario of *period-doubling* → *chaos* (*band splitting*) → *chaos* (*band merging*) again, albeit at a much smaller scale. Same findings are encountered at all the other periodic windows, including miniature windows within the larger windows, as evidence of self-similarity.

3.2 The logistic map with delay

In 1948 Hutchinson [27] introduces a delay in the logistic equation to improve its applications in the study of population dynamics. The proposed model by Hutchinson has been applied in population dynamics [28], deterministic chaotic systems [29], the analysis of random discrete delay equations [30–32], etc. We face a discrete logistic equation with delay [33] given by the difference equation:

$$X_{n+1} = r\, X_n (1 - X_{n-1}), \tag{15}$$

with $0 \leq X_n \leq 1$ and $0 \leq r \leq 2.3$ (r the intrinsic growth). The equation resembles the logistic map (Eq. (13)) saved for the fact that the factor regulating population growth contains a one-generation time delay.

It is convenient to convert the second-order difference equation into an equivalent pair of first-order difference equations. The logistic map with delay is thus recast as a two-dimensional map:

$$\begin{cases} x_{n+1} = r\, x_n (1 - y_n) \\ y_{n+1} = x_n \end{cases}, \tag{16}$$

and the corresponding Lyapunov exponents can be evaluated numerically [26] via

$$\Lambda_1(r) = \lim_{N \to \infty} \frac{1}{2N} \sum_{n=0}^{N-1} \ln \left| \frac{r^2 (1 - y_n - x_n z_n)^2 + 1}{1 + z_n^2} \right|, \tag{17}$$

and

$$\Lambda_1(r) + \Lambda_2(r) = \lim_{N\to\infty} \frac{1}{N} \sum_{n=0}^{N-1} \ln | r \, x_n |, \tag{18}$$

with $z_{n+1} = 1/[r(1 - y_n - x_n z_n]$. In the previous equations, N is the number of iterations.

The pertinent bifurcation diagram and the corresponding Lyapunov exponents Λ_1 and Λ_2 are displayed in **Figure 2a** and **2b**, as a function of the parameter $0 \leq r \leq 2.3$ with $\Delta r = 0.0005$, respectively. We evaluated numerically the delayed logistic map starting from a random initial condition. The first $N_0 = 10^5$ iterations are disregarded (transitory states), and the next $N = 10^6$ ones are used for Lyapunov evaluation (Eqs. (15) and (16)) and information theory quantifiers (Eqs. (3), (5) and (7)).
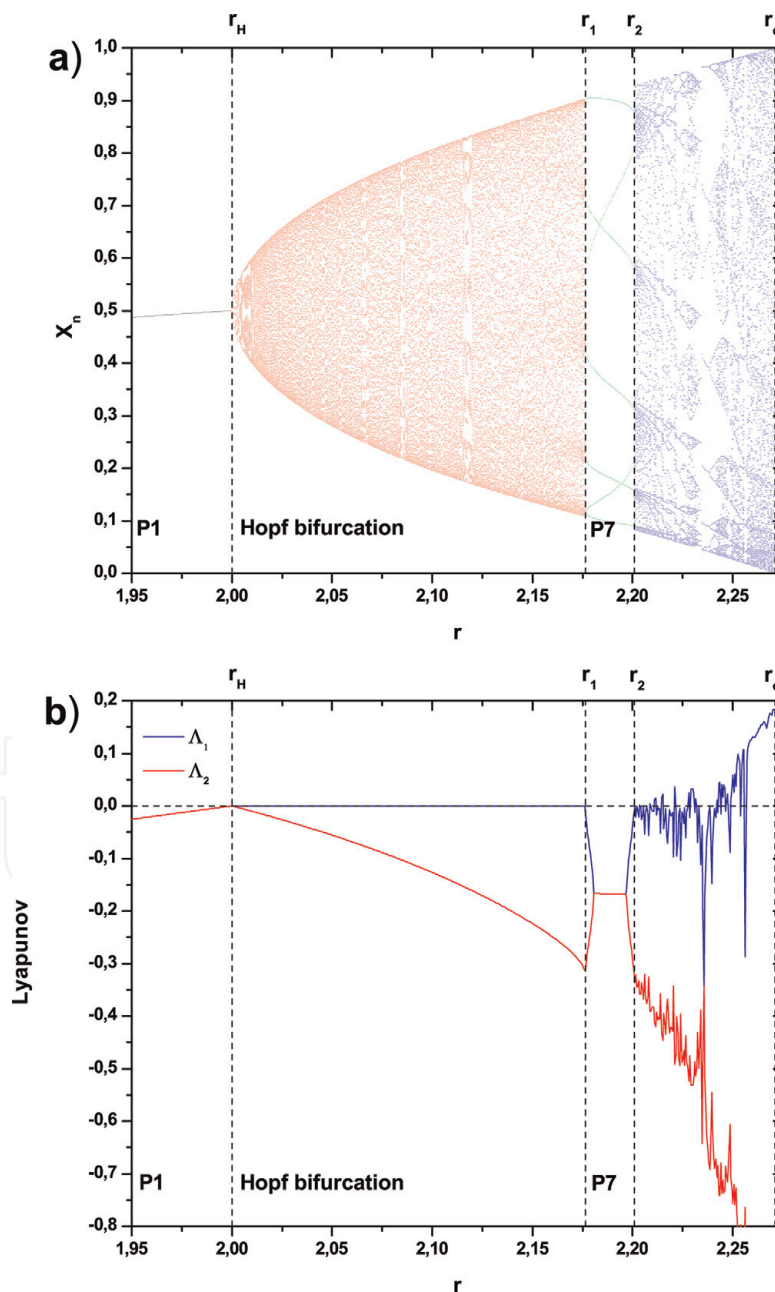
Figure 2.
(a) Bifurcation diagram and (b) Lyapunov exponents Λ_1 and Λ_2 for the delayed logistic map as function of parameter r ($\Delta r = 0.0005$). The vertical segment lines delimited the different dynamical windows described in the text.

This map has common characteristics with the usual logistic map. In particular, $X = 0$ is a fixed point for $r \in [0, 1)$, and $X_n = 1 - 1/r$ is a stationary state for $\in [1, r_H)$. In the delayed logistic map case, when the parameter value is $r_H = 2$, the system shows a Poincare-Andronov-Hopf bifurcation (see **Figure 2**). The quasiperiodic behavior persists over most of the range $r \in [r_H, r_1)$. A seven-cycle periodicity is observed for $r \in [r_1, r_2)$ (with $r_1 = 2.17640$ and $r_2 = 2.20071$). For the parameter $r \in [r_2, r_c)$, one mainly detects chaotic dynamics interspersed with regions of relative simplicity. For $r > r_c = 2.271$, the finite solutions are destabilized, and the system experiences a transition to $-\infty$. In the bifurcation diagram (see **Figure 2a**), it is difficult to distinguish quasiperiodicity from chaos, but the plot displaying Lyapunov exponents (see **Figure 2b**) indicates quasiperiodicity in the region where $\Lambda_1 = 0$.

4. Results and discussion

For each chaotic map previously described, the same time series of length $N = 10^6$ data, used for evaluating the corresponding Lyapunov exponents at each parameter value, are used now to build a Bandt-Pompe PDF (Π), taking an embedding dimension $D = 6$ and time lag $\tau = 1$. Then corresponding time causal information theory quantifiers, normalized Shannon entropy ($H[\Pi]$), statistical complexity ($C[\Pi]$), and Fisher information measure ($F[\Pi]$), were evaluated.

For ordinal entropic quantifiers of Shannon kind (global quantifiers), the BP-PDF provides univocal prescription. However, some ambiguities arise in the case in which one wishes to employ the BP-PDF to construct local quantifiers. The local sensitivity of the Fisher information measure for discrete PDFs is reflected in the fact that the specific "i-ordering" of the discrete values $p(\pi_i)$ must be taken into account in evaluating Eq. (5). If we are working with BP-PDF and consider patterns of length D, we will have $D!!$ possibilities for the i-ordering. We follow the Lehmer lexicographic order [34] in the generation of BP-PDF, because it provides the best graphic separation of different dynamics in the causal Shannon-Fisher plane [13, 24]. We display in **Figures 3** and **4** the causal information quantifiers (entropy, complexity and Fisher) as a function of the parameter r for the logistic map (see **Figure 1**) and delayed logistic map (see **Figure 2**), respectively. In these figures, the different dynamical zones and corresponding colors are both used in the original bifurcation diagrams (**Figures 1a** and **2a**).

For the logistic map, the period-doubling zone is detected for all the quantifiers. In particular for $r < r_\infty$, low entropy and complexity values and maximum Fisher value are found with the different periodic behaviors. A jump in the entropy and complexity value and a drop in Fisher value are observed when period doubling happens. This quantifier behavior is due to for periodic sequences the BP-PDF consisting of a very few $p(\pi_i) \neq 0$ values.

After r_∞ the dynamic becomes chaotic (positive Lyapunov exponent). An abrupt entropy and complexity growth and Fisher decreasing values are observed for $r > r_\infty$ reaching their maximum value at $r = 4$, where we face a totally developed chaotic dynamics. The several "drops" in the entropy and complexity, with the "jumps" in the Fisher values in the parameter interval $r_\infty < r \leq 4$, correspond to the periodic windows as can be easily confirmed compared with the bifurcation and Lyapunov exponent (see **Figure 1**).

For the delayed logistic map, a regular dynamic (steady state) is observed for parameter in the range $r < r_H$ and then has entropy and complexity null values and Fisher maximum value. For $r > r_H$ an oscillatory behavior appears, which is Hopf
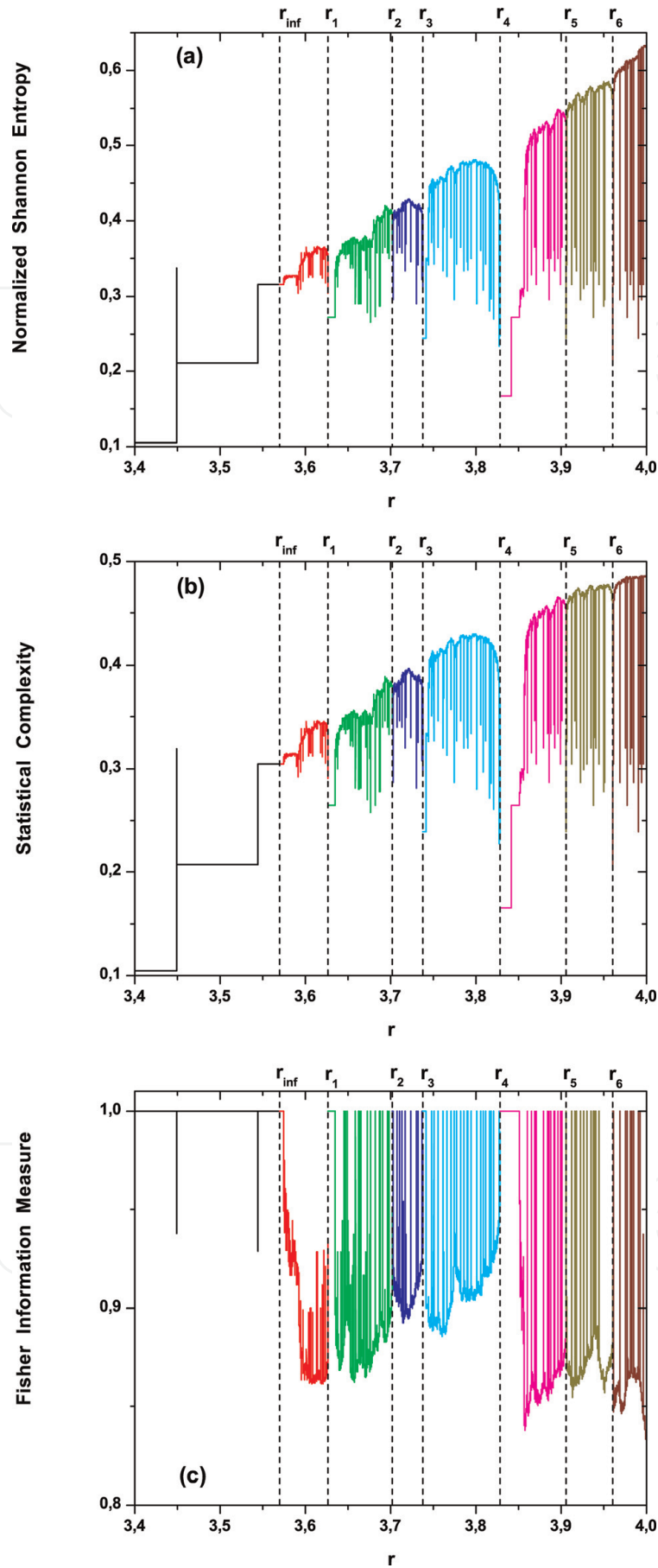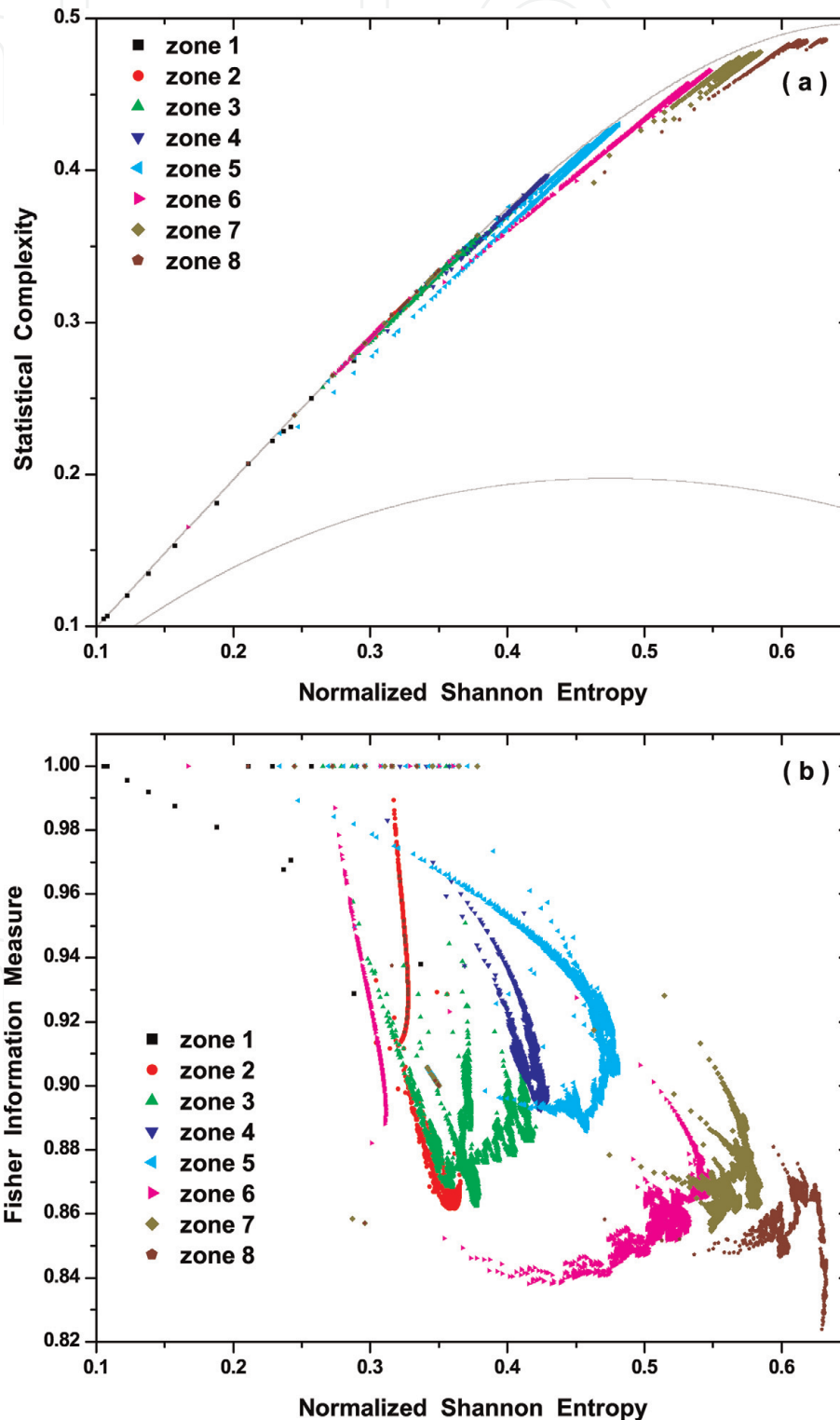
Figure 3.
Time causal information quantifiers for logistic map time series ($M = 10^6$ data) as a function of the parameter r ($\Delta r = 0.0005$): (a) italicized Shannon entropy; (b) statistical complexity; and (c) Fisher information measure, evaluated with Bandt-Pompe PDF, with $D = 6$, $\tau = 1$. The vertical segment lines delimited the different dynamical windows described in the text. The color code for the different zones is the same as in Figure 1a.
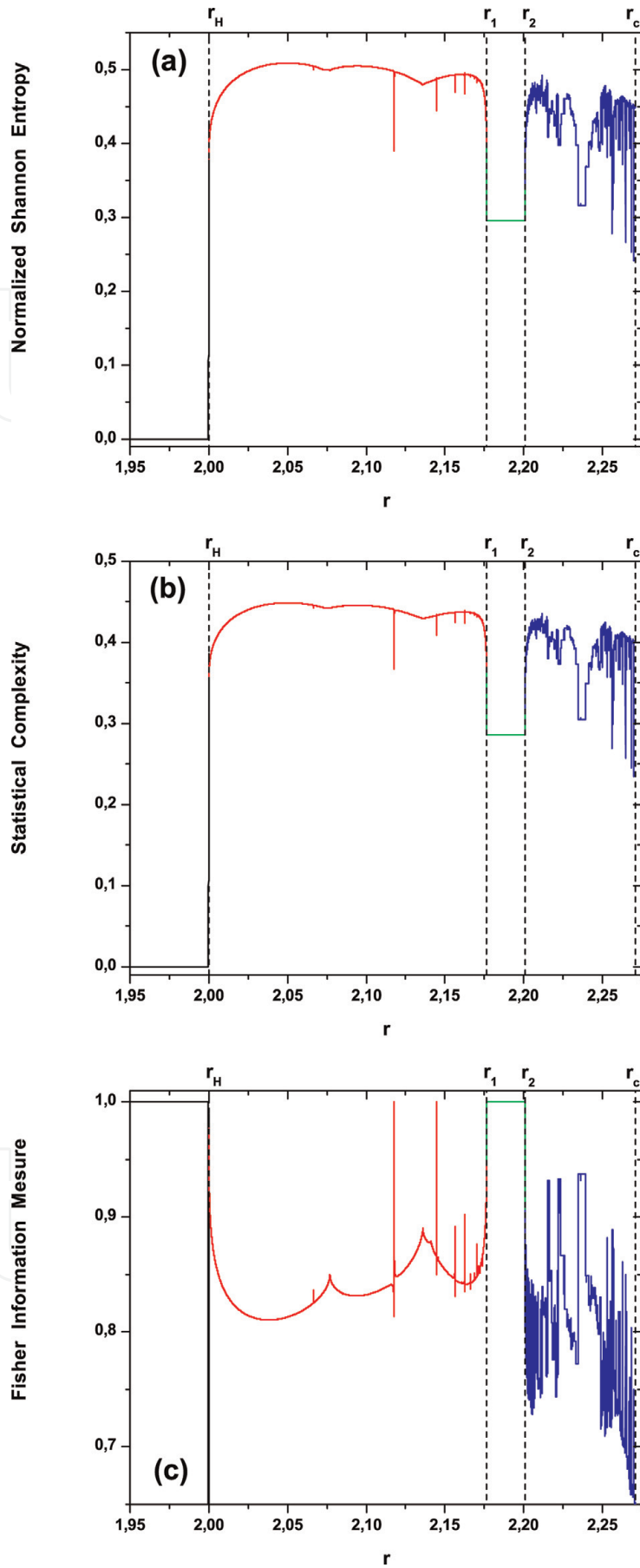
Figure 4.
*Time causal information quantifiers for delayed logistic map time series ($M = 10^6$ data) as function of the parameter r ($\Delta r = 0.0005$): (a) italicized Shannon entropy; (b) statistical complexity; and (c) Fisher information measure, evaluated with Bandt-Pompe PDF, with $D = 6$ and $\tau = 1$. The vertical segment lines delimited the different dynamical windows described in the text. The color code for the different zones is the same as in **Figure 2a**.*

bifurcation with $\Lambda_1 = 0$. This quasiperiodic orbit can be thought as a mixture of periodic orbits of several different fundamental frequencies. The three quantifiers, entropy, complexity, and Fisher, are able to detect changes in the quasiperiodicity oscillations as a function of r, being Fisher the most sensitive (see **Figure 3b**). The growth in the amplitude of this oscillatory behavior as a function r is not detected by the quantifiers because of the independence of the BP-PDF on the amplitude values. Note that the same number of ordinal patterns ($\sim$30 patterns) is materialized for the whole quasiperiodic behavior, indicating its deterministic nature but not giving

Figure 5.
Time causal information planes for logistic map time series ($M = 10^6$ data) for parameter r ($\Delta r = 0.0005$): (a) causal entropy-complexity plane and (b) causal Shannon-Fisher plane. The color code for the different zones is the same as in **Figure 1a**.

indications about the type of dynamics. For the parameter values $r_1 \leq r \leq r_2$, a period 7 window with $H = 0.299576$, $C = 0.288624$, and $F = 1$ is observed. In the parameter range $r_2 \leq r < r_c$, chaotic dynamics with some periodic windows is observed, characterized by higher values of entropy and complexity and lower values of Fisher, in relation to those previously obtained for the period 7 window.

The causal planes $H \times C$ and $H \times F$ for the logistic map in the parameter range $3.4 \leq r \leq 4.0$ are shown in **Figure 5a** and **5b**, respectively. Both planes provide a
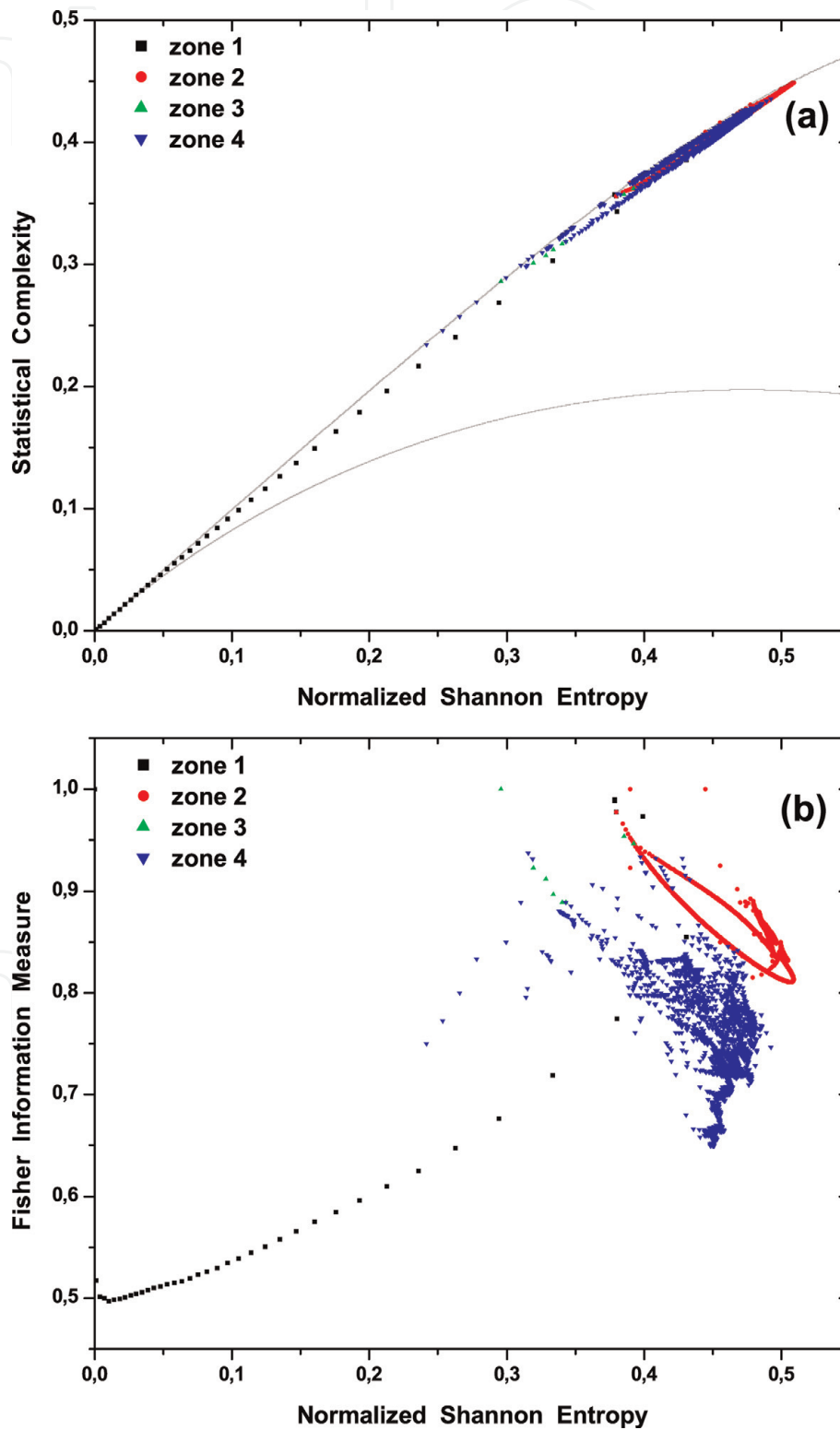
Figure 6.
*Time causal information planes for delayed logistic map time series ($M = 10^6$ data) for parameter r ($\Delta r = 0.0005$): (a) causal entropy-complexity plane and (b) causal Shannon-Fisher plane. The color code for the different zones is the same as in **Figure 2a**.*

characterization of the intrinsic information of the system, independently of the control parameter. From the causal plane $H \times C$ (**Figure 5a**), we can observed that the variation in the whole range of the parameter r locates the system very close to the maximum complexity curve C_{max}, reaching at $r = 4$ (totally developed chaos) and its maximum value $C = 0.48425$. Note also that low entropy values $H < 0.3$ correspond to periodic behavior values; however, these values have also associated high values of complexity with curve C_{max}, making difficult in this way the clear separation of the different dynamic behaviors, but a quantification of the global complexity of the logistic map is obtained. The causal plane $H \times F$ (see **Figure 5b**) shows a clear characterization of the various associated dynamics to different values of the control parameter r, locating them in different zones of the plane. It is in this instance, in which the Fisher permutation reveals its local character and, simultaneous with the global information delivered by Shannon entropy, gives us a sort of "topographical" plane of the dynamics.

In **Figure 6**, we show the behavior of the delayed logistic map for the whole range of the parameter r in the two causality planes. It is clearly that the $H \times C$ plane (**Figure 6a**) gives us just the information of the complexity of the map, which reaches the maximum curve (C_{max}), but does not differentiate between a Hopf bifurcation and the chaotic dynamics developed for $r > r_2$. On the other hand in the $H \times F$ plane (**Figure 6b**), one obtains a good defined structure for the quasiperiodic orbits, due to the oscillations in the quantifiers. The shapeless blue points for $r_2 < r < r_c$ is due to neither the H and the F are not detecting any kind of intermittency or bifurcation that can be present into the chaotic dynamic, at the present parameter resolution Δr.

5. Conclusions

We have shown that taken as starting point a probabilistic description of dynamical system considering the inherent temporal causality in the generated time series throughout Bandt-Pompe methodology, it is possible to evaluate information quantifiers of global or local character and a complete and detailed characterization of the dynamical system can be successfully archived with reference to an information causal plane, in which the two coordinate axes are different information quantifiers. The causal information planes defined are the global-global $H \times C$ plane and the global-local $H \times F$ plane, in which (i) the permutation normalized Shannon entropy ($H[\Pi]$) and the permutation statistical complexity ($C[\Pi]$) are responsible for the global features and (ii) the permutation Fisher information measure ($F[\Pi]$) accounts for the local attributes (all the information quantifiers are evaluated using BP-PDF denoted by Π).

For the discrete systems considered here, the logistic map and the delayed logistic map, we find that both H and C show a correspondence with one of the classic measures of chaoticity, the maximum exponent of Lyapunov, while the local sensitivity of F reveals details of the dynamics, invisible to the other quantifiers. The visualization of the location of the dynamics of the system under analysis, in the information planes, allows us to account for (a) the complexity of the system and (b) characterization of different dynamics in different locations of the plane, enabling the identification of different routes to chaos.

Author details

Felipe Olivares[1], Lindiane Souza[2], Walter Legnani[3] and Osvaldo A. Rosso[2,4]*

1 Instituto Física, Pontificia Universidad Católica de Valparaíso (PUCV), Valparaíso, Chile

2 Instituto Física, Universidad Federal de Alagoas (UFAL), Maceió, Brazil

3 Signals and Images Processsing Center (CSPSI), Facultad Regional Buenos Aires, Universidad Tecnológica Naciona (UTN), Ciudad Autónoma de Buenos Aires, Argentina

4 Instituto de Medicina Traslacional e Ingeniería Biomedica (IMTIB), Hospital Italiano de Buenos Aires (HIBA), CONICET, Ciudad Autónoma de Buenos Aires, Argentina

*Address all correspondence to: oarosso@gmail.com

IntechOpen

References

[1] Kolmogorov AN. A new metric invariant for transitive dynamical systems and automorphisms in Lebesgue spaces. Doklady Akademii Nauk SSSR. 1959;**119**:861-864

[2] Sinai YG. On the concept of entropy for a dynamical system. Doklady Akademii Nauk SSSR. 1959;**124**:768-771

[3] Pesin YB. Characteristic Lyapunov exponents and smooth ergodic theory. Russian Mathematical Surveys. 1977;**32**: 55-114

[4] Abarbanel HDI. Analysis of Observed Chaotic Data. New York, USA: Springer-Verlag; 1996

[5] Gray RM. Entropy and Information Theory. Berlin-Heidelberg, Germany: Springer; 1990

[6] Shannon C, Weaver W. The Mathematical Theory of Communication. Champaign, IL: University of Illinois Press; 1949

[7] Brissaud JB. The meaning of entropy. Entropy. 2005;**7**:68-96

[8] Fisher RA. On the mathematical foundations of theoretical statistics. Philosophical Transactions of the Royal Society of London. Series A. 1922;**222**: 309-368

[9] Frieden BR. Science from Fisher information: A Unification. Cambridge: Cambridge University Press; 2004

[10] Zografos K, Ferentinos K, Papaioannou T. Discrete approximations to the Csiszár, Renyi, and Fisher measures of information. Canadian Journal of Statistics. 1986;**14**: 355-366

[11] Pardo L, Morales D, Ferentinos K, Zografos K. Discretization problems on generalized entropies and R-divergences. Kybernetika. 1994;**30**: 445-460

[12] Sánchez-Moreno P, Yáñez R, Dehesa J. Discrete densities and Fisher information. In: Proceedings of the 14th International Conference on Difference Equations and Applications. Istanbul, Turkey: Ugur-Bahçesehir University Press; 2009. pp. 291-298

[13] Olivares F, Plastino A, Rosso OA. Contrasting chaos with noise via local versus global information quantifiers. Physics Letters A. 2012;**376**:1577-1583

[14] López-Ruiz R, Mancini HL, Calbet X. A statistical measure of complexity. Physics Letters A. 1995;**209**:321-326

[15] Lamberti PW, Martín MT, Plastino A, Rosso OA. Intensive entropic non-triviality measure. Physica A: Statistical Mechanics and Its Applications. 2004; **334**:119-131

[16] Martín MT, Plastino A, Rosso OA. Generalized statistical complexity measures: Geometrical and analytical properties. Physica A: Statistical Mechanics and Its Applications. 2006; **369**:439-462

[17] Bandt C, Pompe B. Permutation entropy: A natural complexity measure for time series. Physical Review Letters. 2002;**88**:174102

[18] Kowalski AM, Martín MT, Plastino A, George Judge G. On extracting probability distribution Information from time series. Entropy. 2012;**14**: 1829-1841

[19] Saco PM, Carpi LC, Figliola A, Serrano E, Rosso AO. Entropy analysis of the dynamics of EL Niño/Southern Oscillation during the Holocene. Physica A: Statistical Mechanics and Its Applications. 2010;**389**:5022-5027

[20] Kowalski A, Martín MT, Plastino A, Rosso AO. Bandt-Pompe approach to the classical-quantum transition. Physica D: Nonlinear Phenomena. 2007;**233**:21-31

[21] Amigó JM, Zambrano S, Sanjuán MAF. True and false forbidden patterns in deterministic and random dynamics. Europhysics Letters. 2007;**79**:50001

[22] Amigó JM. Permutation Complexity in Dynamical Systems. Berlin, Germany: Springer-Verlag; 2010

[23] Rosso OA, Larrondo HA, Martín MT, Plastino A, Fuentes MA. Distinguishing noise from chaos. Physical Review Letters. 2007;**99**: 154102

[24] Olivares F, Plastino A, Rosso OA. Ambiguities in the Bandt and Pompe's methodology for local entropic quantifiers. Physica A: Statistical Mechanics and Its Applications. 2012; **391**:2518-2526

[25] Rosso OA, Olivares F, Plastino A. Noise versus chaos in a causal Fisher-Shannon plane. Papers in Physics. 2015; 7:070006

[26] Sprott JC. Chaos and Time Series Analysis. Oxford: Oxford University Press; 2004

[27] Hutchinson GE. Circular casual systems in ecology. Annals of New York Academy of Sciences. 1948;**50**:221-246

[28] Pounder JR, Rogers TD. The geometry of chaos: Dynamics of a nonlinear second order difference equation. Bulletin of Mathematical Biology. 1980;**42**:551-597

[29] Aronson DG, Chory MA, Hall GR, McGehee RP. Bifurcations from an invariant circle for two-parameter families of maps of the plane: A computer-assisted study. Communications in Mathematical Physics. 1982;**83**:303-354

[30] Cabrera JL, De La Rubia FJ. Numerical analysis of transient behavior in discrete random logistic equation with delay. Physics Letters A. 1995;**197**: 19-24

[31] Cabrera JL, De La Rubia FJ. Analysis of the behavior of a random nonlinear delay discrete equation. International Journal of Bifurcation and Chaos. 1996; **6**:1683-1690

[32] Cabrera JL, De La Rubia FJ. Resonance-like phenomena induced by exponentially correlated parametric noise. Europhysics Letters. 1997;**39**: 123-128

[33] Morimoto Y. Hopf bifurcation in the nonlinear recurrence equation $x_{t+1} = a\, x_t\,(1-x_{t-1})$. Physics Letters A. 1988;**13**: 179-182

[34] Schwarz K. The Archive of Interesting Code. 2011. Available from: http://www.keithschwarz.com/interesting/code/?dir=factoradic-permutation